Boundary Condition Effects on the Dynamic and Electric Properties of Hydration Layers

ARTICLE *in* THE JOURNAL OF PHYSICAL CHEMISTRY A · MARCH 2015

Impact Factor: 2.69 · DOI: 10.1021/jp511824t · Source: PubMed

4 AUTHORS, INCLUDING:

Subramanian Chandramouli

Scuola Normale Superiore di Pisa

13 PUBLICATIONS **97** CITATIONS

SEE PROFILE

Costantino Zazza

Scuola Normale Superiore di Pisa

38 PUBLICATIONS **371** CITATIONS

SEE PROFILE

Giordano Mancini

Scuola Normale Superiore di Pisa

56 PUBLICATIONS **530** CITATIONS

SEE PROFILE

THE JOURNAL OF PHYSICAL CHEMISTRY A

Article

pubs.acs.org/JPCA

Boundary Condition Effects on the Dynamic and Electric Properties of Hydration Layers

Balasubramanian Chandramouli,[†] Costantino Zazza,[†,§] Giordano Mancini,[†,‡] and Giuseppe Brancato*[,†,‡]

[†]Scuola Normale Superiore, Piazza dei Cavalieri 7, I-56126 Pisa, Italy

[‡]Istituto Nazionale di Fisica Nucleare (INFN) Sezione di Pisa, Largo Bruno Pontecorvo 3, 56127 Pisa, Italy

ABSTRACT: Water solvation has a central role in several biochemical processes ranging from protein folding to biomolecular recognition and enzyme catalysis. Because of its importance, the structure and dynamics of hydration layers around biological macromolecules have been the targets of a great number of experimental and computational studies. In the present contribution, we have investigated the effects of periodic boundary conditions (PBCs), as used in conjunction with molecular dynamics (MD) simulations, on the dynamic and electric properties of water layers. In particular, we have systematically performed MD simulations of neat water and biomolecules in aqueous solutions by imposing a different external dielectric constant, a generally overlooked parameter in PBC simulations. The effect of the system size has also been addressed. Overall, our results consistently indicate that the dipole moment properties of water layers, and specifically the dipole moment fluctuations and the reorientational correlation functions, can be sensitive to the choice of the external boundary conditions, whereas other molecular properties, such as the self-diffusion coefficient and the reorientational relaxation times, are not affected. We think that our investigation may help to assess appropriate simulation conditions for modeling the aqueous environment of relevant biochemical systems and processes.

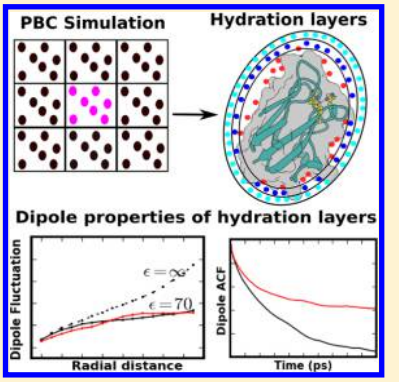

1. INTRODUCTION

Water plays a crucial role in all biological phenomena, ranging from the stabilization of protein structures to the participation in enzymatic reactions and ligand/substrate binding to proteins.[1] The ability of water to form three-dimensional networks of hydrogen bonds and to effectively screen charged species is also a key feature for the control of biomolecular functions, e.g., mediating the molecular recognition processes.[2−5] Several experimental techniques have been developed to gain information on the structural and dynamic properties of water localized in the hydration layers of biomolecules, such as NMR relaxation experiments,[6] linear and nonlinear vibrational spectroscopy,[7,8] and time-resolved fluorescence spectroscopy.[9] Accordingly, a number of water interfacial properties have been estimated, including translational and rotational motions, collective interfacial modes, water exchange among solvation shells, and water density profiles at the surface of biomolecules. More recently, terahertz dielectric measurements[10,11] allowed more detailed information to be gained on the electrostatic properties of water around proteins, including solvent polarization and dynamics of the nearest solvation shells of biological macromolecules extending up to 15−20 Å into bulk water. As a complementary approach, molecular dynamics (MD) simulations are largely used to provide atomistic level insights into the dynamical behavior of biomolecules and are routinely used to study solvent dynamic effects,[12,13] since several physicochemical properties of complex molecular systems can be directly or indirectly computed.[14,15] Indeed, simulations of biomolecules in explicit solvent ranging from nanosecond to millisecond time scales are routinely performed, thanks to the advances of both computer architectures and algorithms.[16] However, the reliability of the MD trajectories depends on numerous parameters, such as the reliability of the force fields, the stability of the numerical integrator, the soundness of the thermostat/pressure couplings, the treatment of the boundary conditions, the influence of finite size effects, etc. Therefore, a careful assessment of all such MD ingredients is a mandatory requirement in order to obtain meaningful and, possibly, accurate estimates of the observables under investigation. Most commonly, MD simulations of biosystems are carried out enforcing periodic boundary conditions (PBCs) in combination with Ewald lattice sum techniques,[14,17] where identical images of a central explicit system are replicated in all three spatial directions and embedded into a dielectric continuum at infinity, thus avoiding the unphysical modeling of a biosystem in a vacuum (even if preliminarily solvated with a few water layers) and providing a satisfactory representation of the system under typical experimental conditions. Such a simulation methodology has several advantages over other methods,[18−21] primarily an effective and reliable evaluation of the long-range electrostatics interactions and the absence of spurious boundary effects at the simulation cell edges. However, PBCs are not free of possible

Special Issue: Jacopo Tomasi Festschrift

Received: November 26, 2014
Revised: February 18, 2015

DOI: 10.1021/jp511824t
J. Phys. Chem. A XXXX, XXX, XXX−XXX

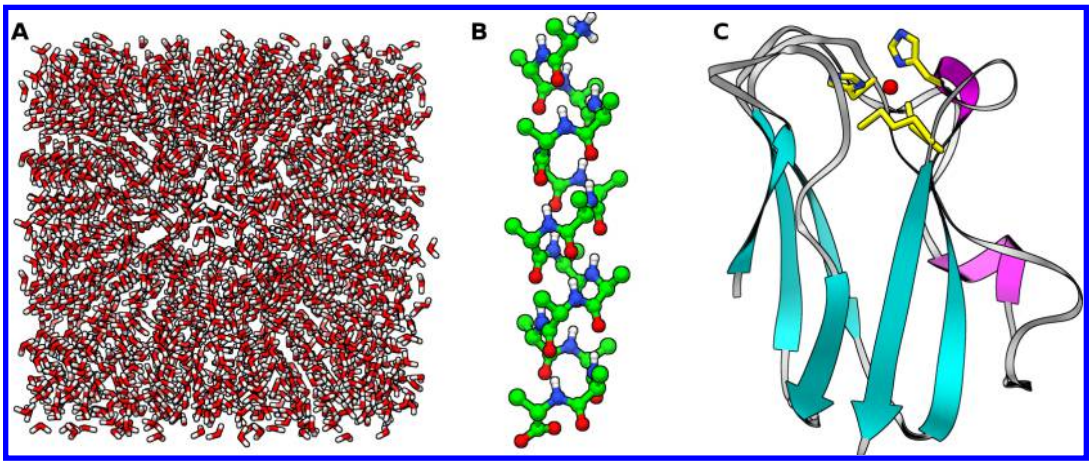

Figure 1. Pictorial representations of the simulated systems: (A) pure water, (B) hexadeca alanine peptide (Ala16), and (C) plastocyanin copper-protein. Plastocyanin is depicted as a ribbon, colored on the basis of the secondary structure. The Cu(II) ion is shown in red, and the protein residues bound to copper are shown in yellow.

artifacts, and some issues related to the artificially imposed periodicity have been reported in a number of previous studies (e.g., possible inconsistencies on the ion distributions, conformational equilibria, and energetic bias in the simulated ensemble).[22−31] While, for example, alternative methods based on continuum models have been proposed in the literature,[32−38] as successfully applied in the framework of quantum chemistry (e.g, the polarizable continuum model developed by Jacopo Tomasi and collaborators[39,40]), none has received the same general consensus of the PBC/Ewald lattice sum in the context of MD simulations of large and complex biosystems. Among others, one ingredient in PBC simulations that is often overlooked and might need further examination concerns the treatment of the PBC dielectric continuum and its subtle effects on water dipole properties, especially in proximity of complex and rugged surfaces, such as those featured by biological macromolecules: it is worth noting that in most common MD codes the dielectric continuum is modeled by a predefined relative permittivity (dielectric constant), not readily accessible from input keywords. This is even more relevant in view of the recent applications of advanced spectroscopic techniques[10,11] to the investigation of water layers in biological environments. Interestingly, the choice of the PBC dielectric continuum has been shown to affect the stabilization energy of different ice nanocrystals, as obtained by high-level quantum mechanical calculations.[41]

In the present work, we aim at studying the effects of the external dielectric medium, in terms of its relative permittivity, on the dynamical properties of hydration layers in typical PBC simulations of biomolecules in aqueous solutions. To this end, we have chosen three aqueous systems of increasing complexity: (i) neat water, (ii) a hexadeca alanine peptide, and (iii) plastocyanin, a well-known copper-containing protein (Figure 1). MD simulations of these systems have been performed under PBCs with two external dielectric constants, which, for convenience, are indicated as the highly conducting ($\varepsilon_{ext} = \infty$) and the low-dielectric ($\varepsilon_{ext} = 70$) medium: the former is generally known as tinfoil conditions, perhaps the most widespread adopted choice with Ewald lattice sum techniques, while the latter corresponds to the relative permittivity of a typical water model (SPC[42]) under normal conditions. In addition, the effects of system size and solute flexibility on the water properties in response to the boundary treatment have been addressed. In particular, we have analyzed in detail water polarization, dipole moment fluctuations (DMFs), reorientational dynamics, and water mobility on selected hydration layers at various distances from biomolecule surfaces.

The paper is organized as follows: In section 2, computational details on the molecular models, simulation methods, and analyses are provided and described in some detail. In the Results and Discussion section, we report on the simulations of neat water, alanine peptide, and plastocyanin in aqueous solution, where water layer analyses and results are thoroughly discussed. Conclusions are given in the last section (section 4).

2. METHODS

2.1. Computational Details. All simulations were performed in a NVT ensemble using two distinct values for the external dielectric constant ($\varepsilon_{ext} = \infty$ or 70) for a time interval sufficient to achieve the convergence of the investigated water properties with periodic boundary conditions (see Table 1). The particle-mesh Ewald (PME)[43] method was used to treat long-range electrostatics (Fourier grid spacing, 0.1 nm; PME interpolation order, 6). Note that, within the Ewald sum formalism, an additional energetic coupling term has to be included when dealing with a low dielectric continuum, which generally depends on simulation cell shape and external dielectric constant.[44] In this study, the present coupling term has the form

$$U = \frac{2\pi}{(2\varepsilon_{ext} + 1)V}\mathbf{M}^2 \quad (1)$$

where $\mathbf{M}$ is the instantaneous total dipole moment of the sample and V is the cell volume. Bonds containing hydrogen

Table 1. Summary of the MD Simulation Details

system	no. of water	ε_{ext}	box size (Å)	time (ns)
water[a]	2170	∞, 70	40	30
water	11423	70	70	30
Ala16	1508	∞, 70	50	30
Ala16	5804	∞, 70	70	30
plastocyanin	8817	∞, 70	70	60

[a]A smaller water box has been simulated with SPC, SPC/E, and TIP3P water models.

DOI: 10.1021/jp511824t
J. Phys. Chem. A XXXX, XXX, XXX−XXX

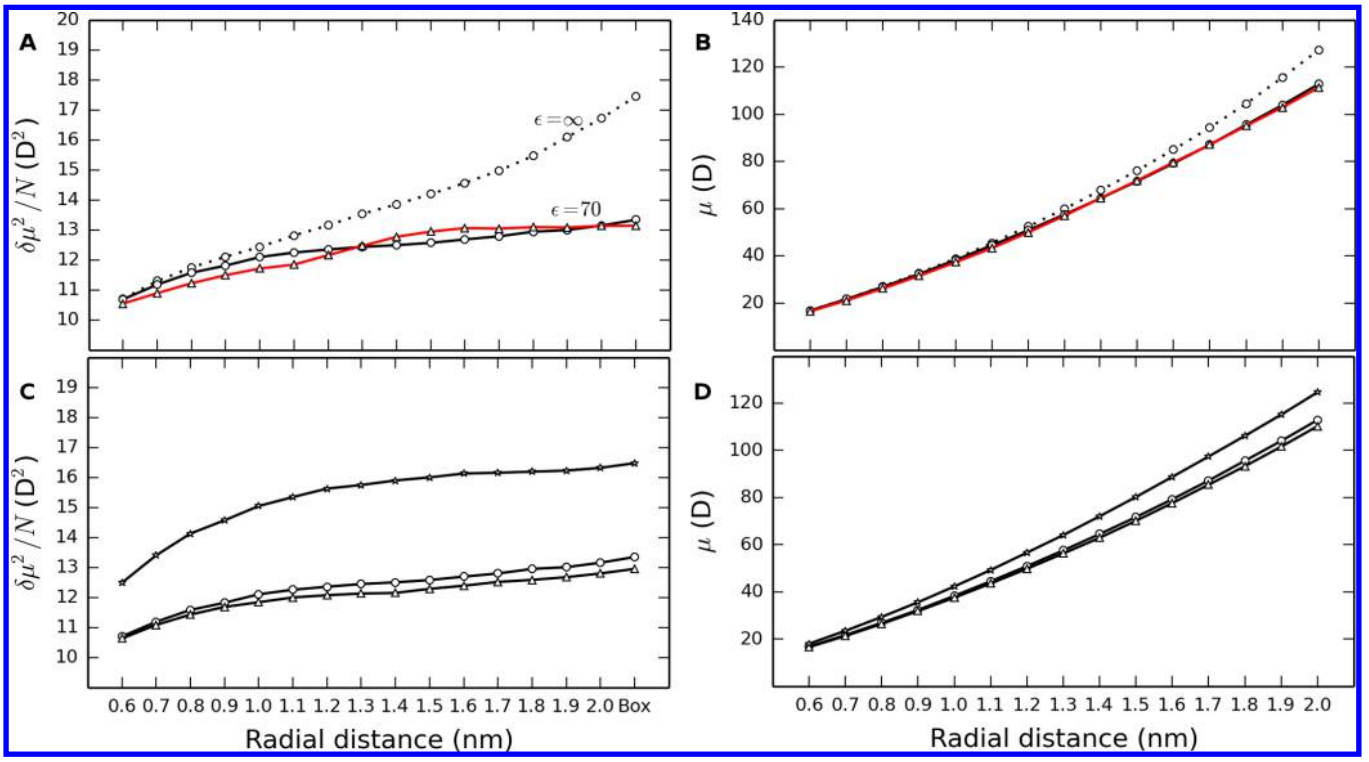

Figure 2. (A) Normalized dipole moment fluctuations ($\delta\mu^2$) and (B) average dipole moment (μ) of SPC water as a function of the spherical radius (nm): solid black line, small water system (40 Å edge) and ε_{ext} = 70; solid red line, large water system (70 Å edge) and ε_{ext} = 70; dotted black line, small water system and ε_{ext} = ∞. (C) Normalized dipole moment fluctuations and (D) average dipole moment of SPC (circles), SPC/E (triangles), and TIP3P (stars) water models (small water system, ε_{ext} = 70). In panels A and C, standard deviations are about 0.3−0.5.

atoms have been constrained using the LINCS algorithm.[45] A time step of 2 fs and nonbonded cutoff radius of 12 Å were used. Temperature was kept constant at 300 K using the velocity rescaling method[46] with a coupling constant of 0.1 ps during sampling.

Neat water simulations were carried out using cubic simulation cells of two dimensions, 40 and 70 Å edge. In the case of the smaller system, three popular water models were compared, namely, SPC,[42] SPC/E,[47] and TIP3P.[48] As a further test case, SPC water was also simulated according to the general liquid optimized boundary (GLOB)[36−38] model, using a multithreaded parallel version of our in-house simulation code (JERSEY, a MD code developed by CZ and GB) with the same low-dielectric boundary conditions set for the surrounding continuum. The details of the GLOB model are fully described elsewhere.[36−38] The starting coordinates for the hexadeca alanine peptide (hereafter referred to as Ala16) were obtained by building up a conventional right-handed α-helix model using the xleap tool from the AMBER package,[49] with standard COO^- and NH_3^+ terminal groups. Then, the peptide was simulated with the GROMOS96 all-atom force field (43a1)[50] as solvated with SPC water in rectangular simulation cells of different sizes (Table 1). The simulation of the alanine peptide was carried out by freezing the peptide coordinates. Starting coordinates for plastocyanin were obtained from the Protein Data Bank (ID code: 1ag6).[51] Plastocyanin contains a copper coordination site that consists of a Cu(II) ion interacting with four protein residues (His37, His87, Cys84, Met92). The charge and force field parameters for copper and associated protein ligands were taken from a previous simulation study,[52] while standard AMBER ff03[53] parameters were adopted for modeling the rest of the protein. The protein was neutralized with counterions and solvated by TIP3P water in a simulation box extending up to 15 Å from the solute surface. Plastocyanin in aqueous solution was simulated by imposing both fixed and free (unconstrained) protein atomic coordinates. A thermal equilibration was carried out prior to the production simulation as follows: (1) two rounds of minimizations (3500 iterations each) and dynamics (30 ps each) of solvent and counterions with the solute restrained with a force constant of 500, 100, 300, and 50 kcal/(mol Å^2); (2) two rounds of minimization of the whole system with a restraint of 15 and 2 kcal/(mol Å^2) on the protein; and (3) an unrestrained minimization of the whole system. Finally, the system was slowly heated up for about 2 ns from 100 to 300 K at constant volume and equilibrated for a further 1 ns at constant pressure (1 atm). After density equilibration, the NVT production run was carried out. Details of the simulated systems are summarized in Table 1. All simulations were performed using the GROMACS[54] simulation package (version 4.5.4).

2.2. Analysis of the MD Simulations. The electric dipole moment ($\boldsymbol{\mu}$) and corresponding fluctuations ($\boldsymbol{\delta\mu^2} = \langle|\boldsymbol{\mu}|^2\rangle - \langle\boldsymbol{\mu}\rangle^2$) were calculated by considering water solvation layers of increasing size from the simulation cell center (neat water) or from the van der Waals surface of the biomolecule (Ala16 and plastocyanin). All analyses were performed with in-house codes that identified, as a first step, the water molecules at a specific distance with respect to the reference surface, followed by corresponding electrostatic calculations. In addition, water dipole dynamic properties have been analyzed in terms of dipole−dipole autocorrelation functions (ACFs), using a time lag of 20 ps. The obtained ACFs were then fitted to monoexponential functions to estimate relaxation times (note

DOI: 10.1021/jp511824t
J. Phys. Chem. A XXXX, XXX, XXX−XXX

that, due to statistical noise and a likely intrinsic nonexponential relaxation, the fitted correlation times are only used for an approximate quantitative comparison). In addition to such collective water properties, some molecular properties, namely, the self-diffusion coefficient and the rotational relaxation time, were also evaluated using standard tools provided by the GROMACS[54] package. The water self-diffusion coefficient was estimated from the slope of the mean square displacements of solvent molecules versus time.[55] The rotational relaxation time was calculated from the reorientational autocorrelation function expressed as

$$C_l(t) = \langle P_l[\mathbf{e}(t)\cdot\mathbf{e}(0)]\rangle \quad (2)$$

where P_l is the lth rank Legendre polynomial and $\mathbf{e}$ is a unit vector. Here, we considered the first-order Legendre polynomial and the correlation functions of the unit vectors along both the water molecular dipole (μ) and the normal to the molecular plane. The single molecule correlation times (τ^{μ}, $\tau^{\perp}$) were obtained by fitting the correlation function to an exponential function.[56,57] Again, nonexponential relaxations, as well as anomalous diffusion, as observed in other studies,[58] have been discarded in the following comparison of water solvation layers. The molecular models in Figure 1 were created with Chimera,[59] and the graphical plots were made with the matplotlib library.[60]

3. RESULTS AND DISCUSSION

3.1. Dipole Moment Fluctuations and the Dielectric Constant. In the present study, we have analyzed in some detail the dipole moment fluctuations of the hydration shells of different systems as issuing from typical MD simulations of aqueous solutions. It is worth noting that DMFs are of general interest not only for the direct influence on several chemical and physical observables directly or indirectly detectable with modern spectroscopic techniques, as mentioned in the Introduction, but also for the well-known relation with the dielectric constant. Indeed, seminal works by Kirkwood,[61,62] Neumann,[63,64] and others[65] have shown how, from statistical mechanical considerations, the dielectric constant, which is a "macroscopic" property, can be retrieved from the DMFs of a "microscopic" molecular liquid sample by a relatively simple statistical averaging process (the normalized DMFs of a dipolar liquid are also known as the finite-system Kirkwood g-factor in the literature[63]). The latter is an important theoretical result, as well as an illustrative example of the fruitful application of linear response theory, with many practical consequences. For example, it allows the evaluation of the dielectric constant from standard MD simulations without the necessity to resort to the explicit application of an external electric field to the system under investigation. On the other hand, there are some subtleties[63] related to the specific equation that connects DMFs and the dielectric constants of liquids depending on the particular MD methodology employed for the electrostatic long-range calculations (e.g., spherical cutoff radius, cutoff radius + reaction field, or Ewald lattice sum). In the following discussion, we will focus only on DMFs of water shells around different biosystems, for the sake of comparison. Nevertheless, it is worth keeping in mind the present connection with a significant "macroscopic" property, i.e., the dielectric constant.

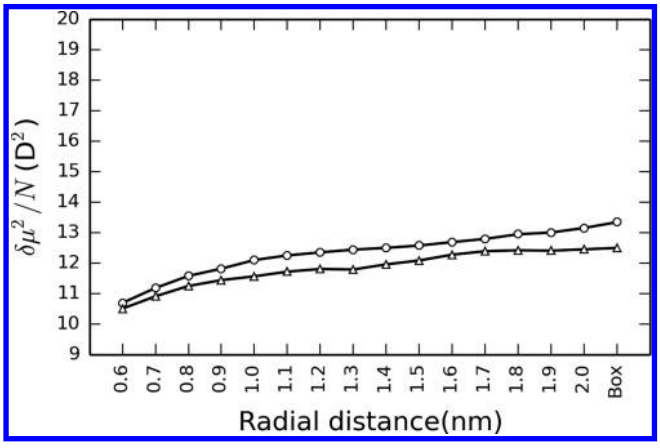

Figure 3. Normalized dipole moment fluctuations ($\delta\mu^2$) of SPC water obtained from PBC (circles, ε_{ext} = 70) and GLOB (triangles) simulations. Standard deviations are about 0.3−0.5.

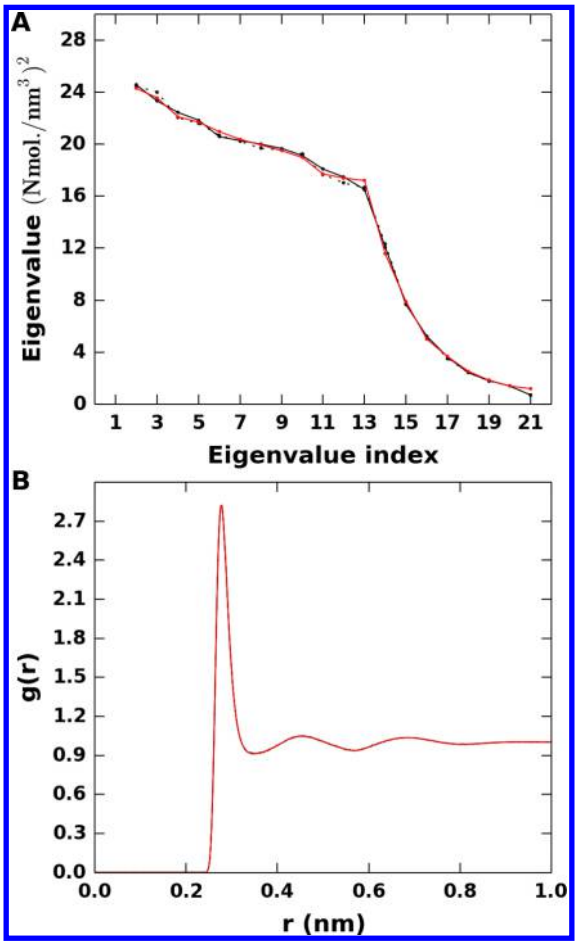

Figure 4. (A) Eigenvalues of the spatial density covariance matrix built from 20 concentric spherical layers having constant volume up to a radius of 2 nm. Data issuing from SPC water small (40 Å) and large (70 Å) systems are shown in black and red, respectively. Dotted and solid black lines represent simulations with ε_{ext} = ∞ and 70, respectively. (B) Radial distribution function of the oxygen atoms of water, represented with the same color scheme as mentioned above.

3.2. Neat Water. Simulations of liquid water under normal conditions (T = 300 K; ρ = 55.3 mol/L) were carried out according to a NVT ensemble by enforcing PBC and using the PME[43] method for the electrostatic interactions. The external dielectric constant of the surrounding medium was set to either ε_{ext} = 70 or ε_{ext} = ∞. The latter value corresponds to the so-

DOI: 10.1021/jp511824t
J. Phys. Chem. A XXXX, XXX, XXX−XXX

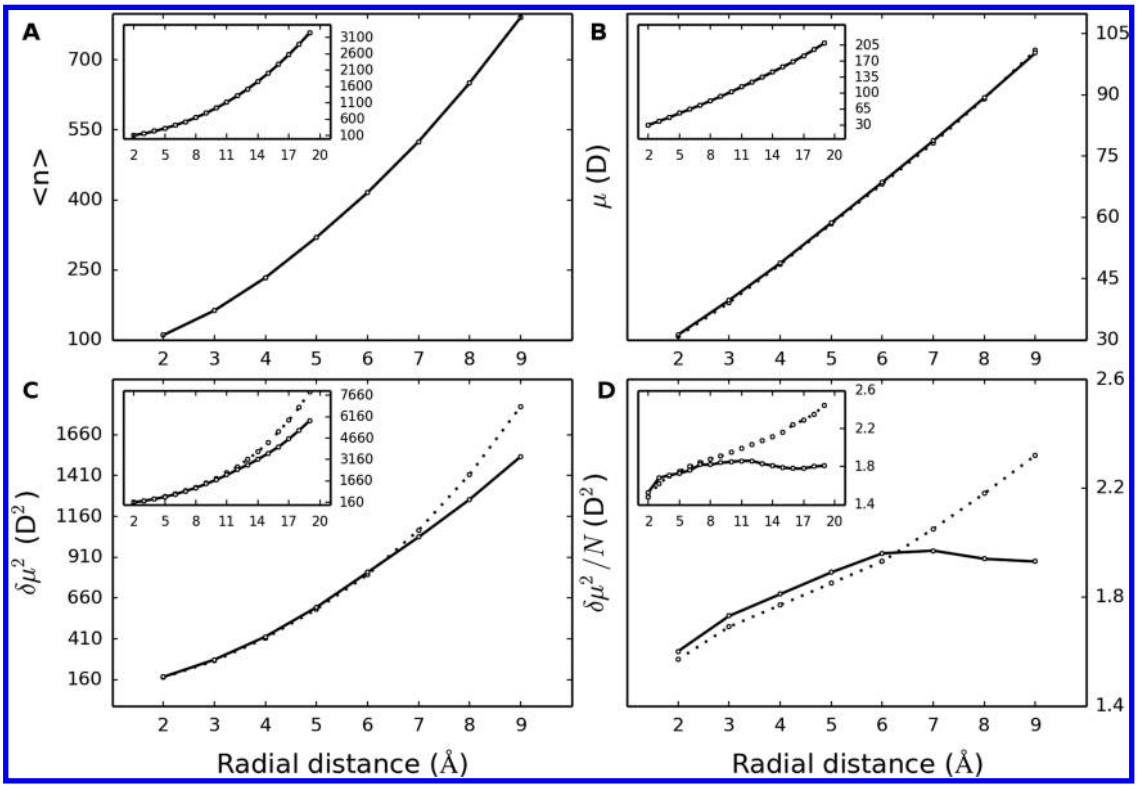

Figure 5. Dipole properties of the hydration layers around hexadeca alanine peptide. (A) Average number of water molecules ($\langle n \rangle$), (B) average dipole moment (μ), (C) dipole moment fluctuations ($\delta\mu^2$), and (D) normalized dipole moment fluctuations of the hydration layers as a function of the distance from the van der Waals surface of the peptide. Dotted and solid lines represent results with ϵ_{ext} set to ∞ and 70, respectively. Data issuing from a larger system are reported in the plot insets.

called tinfoil boundary conditions, which is the standard choice in typical MD simulations of biological systems. On the other hand, ϵ_{ext} = 70 corresponds to the dielectric constant issuing from bulk SPC water simulations, as previously reported,[36] and is rather close to the experimental counterpart (ϵ_r = 78.3). For the sake of comparison, we have considered three rather popular water models routinely used in biosystem simulations, namely, SPC, SPC/E, and TIP3P. Note that SPC and SPC/E share the same geometry but a different electrostatic parametrization, leading to a molecular dipole moment of 2.27 and 2.35 D, respectively. TIP3P is parametrized according to the experimentally determined gas-phase geometry of water but with a dipole moment of 2.35 D to account for molecular polarization in the liquid phase. It should be noted that a similar analysis on pure water was presented in previous studies,[31,36,66] though not purposely tailored versus hydration layer properties; in this work, we have extended such a preliminary and original investigation on liquid water with the aim to complement and better interpret our analysis of biomolecule solvation (vide infra).

The dielectric properties of water were calculated considering spherical layers of increasing size starting from the geometric center of the cubic simulation cell (note that for an homogeneous system, as in this case, the choice of the origin is arbitrary). In Figure 2A, the normalized dipole moment fluctuations ($\delta\boldsymbol{\mu}^2/N$, with N being the number of water molecules) of SPC water as a function of the spherical radius of the selected region are depicted. The profiles of the DMFs show a similar increase up to a radius of ∼1 nm; then, they diverge considerably toward the box edges. In the case of low-dielectric boundaries, the (normalized) DMFs reach a plateau at about 1.2 nm ($\delta\boldsymbol{\mu}^2/N \sim 13$ D^2), which likely corresponds to the thermodynamic (macroscopic) limit of such an observable for the considered water model (SPC). In fact, from a low-dielectric boundary simulation of a larger system carried out to test the system-size effects (see Table 1), we have observed an identical DMF trend (red solid line, Figure 2A), within statistical noise. The DMFs consistently maintain a linear increase with sample size (or constancy of the corresponding normalized quantity) beyond 1.2 nm and until the whole simulation box was considered (i.e., DMFs computed from all water molecules, last data point in Figure 2A). On the other hand, the normalized dipole fluctuations do increase monotonically with size (i.e., spherical radius) when tinfoil boundary conditions are applied; thus, no apparent plateau can be noticed (at least for the system size under consideration). As a consequence, the normalized DMFs do appear significantly different in sample regions greater than 1 nm (radius) and largely different when the whole systems are considered (∼13 D^2 vs ∼18 D^2). Note that boundary condition effects on DMFs have been noted since the original formulation of the Ewald sum techniques (e.g., see ref 65) and a recent study reported other water dipolar properties to be also affected by boundary conditions.[67] However, in these PBC simulation studies, the main focus was on the recovery of the correct water dielectric constant from DMFs rather than on the DMFs *per se*, as in this work.

To further test the physical consistency of the water DMFs issuing from the low-dielectric boundary conditions, an alternative GLOB[36−38] simulation of neat water was purposely carried out and results were compared with PBC ones (see Figure 3). Remarkably, water dipole fluctuations showed the

DOI: 10.1021/jp511824t
J. Phys. Chem. A XXXX, XXX, XXX−XXX

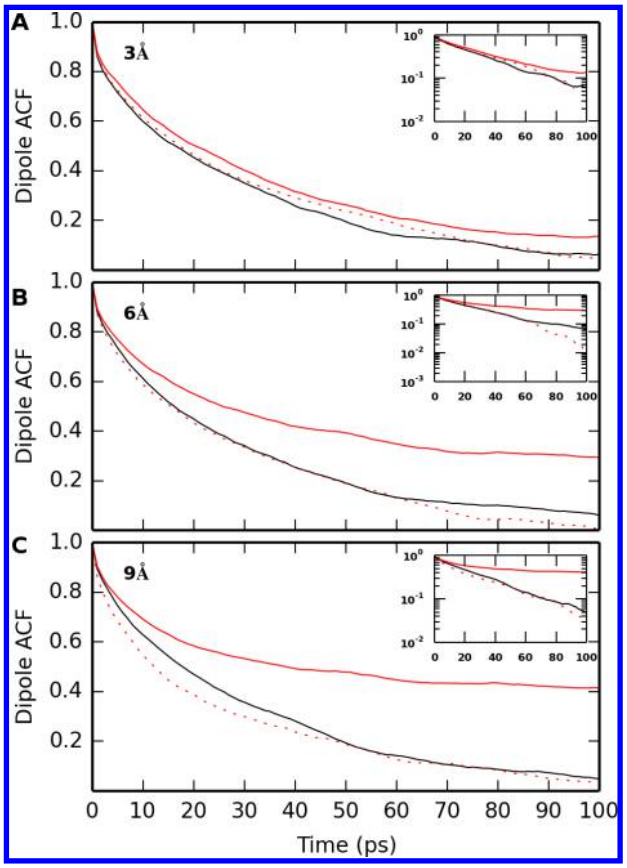

Figure 6. Reorientational autocorrelation functions of the water layer dipole moment issuing from regions of variable thickness (also indicated within each panel) from the alanine peptide surface: (A) hydration layer up to 3.0 Å from the peptide surface, (B) hydration layer up to 6.0 Å, and (C) hydration layer up to 9.0 Å. Solid black line, small system with $\varepsilon_{ext} = \infty$; solid red line, small system with $\varepsilon_{ext} = 70$; dashed red line, large system with $\varepsilon_{ext} = 70$. Semilog plots are reported in the insets.

same asymptotic profile, within statistical noise, reaching a rather similar plateau at about the same spherical region size (1.2−1.4 nm), thus supporting the hypothesis that a genuine (boundary independent) "thermodynamic" limit of $\delta\boldsymbol{\mu}^2/N$ is obtained once a "mesoscopic" liquid sample is considered (N = ∼500).

Furthermore, while DMFs of growing water regions are rather sensitive to the boundary conditions, the averages of the norm of the dipole moments issuing from the same water samples do not significantly differ in a size dependent manner (see Figure 2B). Also, no apparent differences have been observed from further investigations of local structural properties: the O−O radial distribution functions nicely matched each other, and the local density fluctuations showed a very similar eigenvalue analysis (see Figure 4). These results confirmed that the external dielectric constant does not generally introduce any bias in the physical properties of homogeneous systems, as previously noted.[68] In order to validate the consistency of the present results on pure water and the generality of the observed boundary induced effects, a comparative analysis has been carried out with SPC/E and TIP3P water models adopting low-dielectric boundary conditions. The trend in the water dipole moment and corresponding normalized fluctuations of such three-site water models (i.e., SPC, SPC/E, TIP3P) appeared rather similar: again, a plateau beyond 1.2 nm radius has been observed (Figure 2C). However, it should be noted that TIP3P DMFs converged to a higher value as compared to SPC or SPC/E, which can be envisaged to be related to the inherent difference in the dynamic properties of such a model. On a further note, the bulk dielectric constant of TIP3P was estimated to be higher than the other water models (ε = 97[69]), a result consistent with the present observation (see also the discussion in the previous section). In Figure 2D, the average dipole moments evaluated on spherical regions of growing size show no significant discrepancies among the same systems, in line with the similar molecular dipole moments reported above.

3.3. Alanine Peptide. MD simulations of the Ala16 peptide were carried out in an aqueous solution of SPC water with different boundary conditions and box sizes (see the Methods section for details). In this case, a water dipole analysis has been performed considering hydration layers of variable thickness, as a function of the distance from the van der Waals surface of the peptide. Moreover, in order to make a consistent analysis of the water layers, the coordinates of the alanine peptide have been kept frozen during the simulation. In this manner, any misinterpretation of the results has been avoided as related with the definition of the water layers and/or their possible volume variation along the dynamics as a consequence of the peptide conformational rearrangements. Indeed, we believe this is a particularly appropriate choice given that the focus of the present study is on the hydration layer properties (e.g., DMFs), which are generally characterized by time scales matching those of large amplitude protein motions.

In Figure 5, results on the average number of water molecules, the average dipole moment, and the DMFs are depicted. In particular, the average dipole moment of the water layers follows a similar trend in both low-dielectric and high-conducting boundary simulations (Figure 5B). Nevertheless, a rising difference in DMFs is observed upon increasing the distance from the peptide (and corresponding layer thickness) or, in other words, including more surrounding water molecules in a range from 2 to 9 Å. This difference can be better visualized by considering the normalized DMFs (Figure 5D), which does confirm the presence of a plateau in the dipole fluctuations, in the case of ε_{ext} = 70, as we move beyond a distance of 6−7 Å. Note that such a discrepancy does fall already at the level of the second water shell around the peptide, at least partially, and becomes even larger in the following solvation shells. These findings are in analogy to the case of neat water, as described above. Results issuing from Ala16 simulated in a larger simulation cell are depicted in the insets of the corresponding graphical plots of Figure 5. Once again, results have shown differences in the water layer DMFs upon changing the external dielectrics. However, in this case, the divergence in the dipole fluctuations does appear at a longer distance from the solute (at around 11 Å, see inset of Figure 5D) as compared to the simulations of the smaller system (about 7 Å, see Figure 5D). This promptly displays the role of system size (or buffer) on the considered property (i.e., DMFs): extending the simulation cell dimension makes the influence of the boundary conditions gradually less significant on any computed quantity in proximity of the solute−solvent interface, up to the point where the boundary treatment becomes basically irrelevant (in the limit of an extremely large system).

Further, we have investigated the dynamical behavior of the hydration layer dipoles in a similar fashion, i.e., increasing the

DOI: 10.1021/jp511824t
J. Phys. Chem. A XXXX, XXX, XXX−XXX

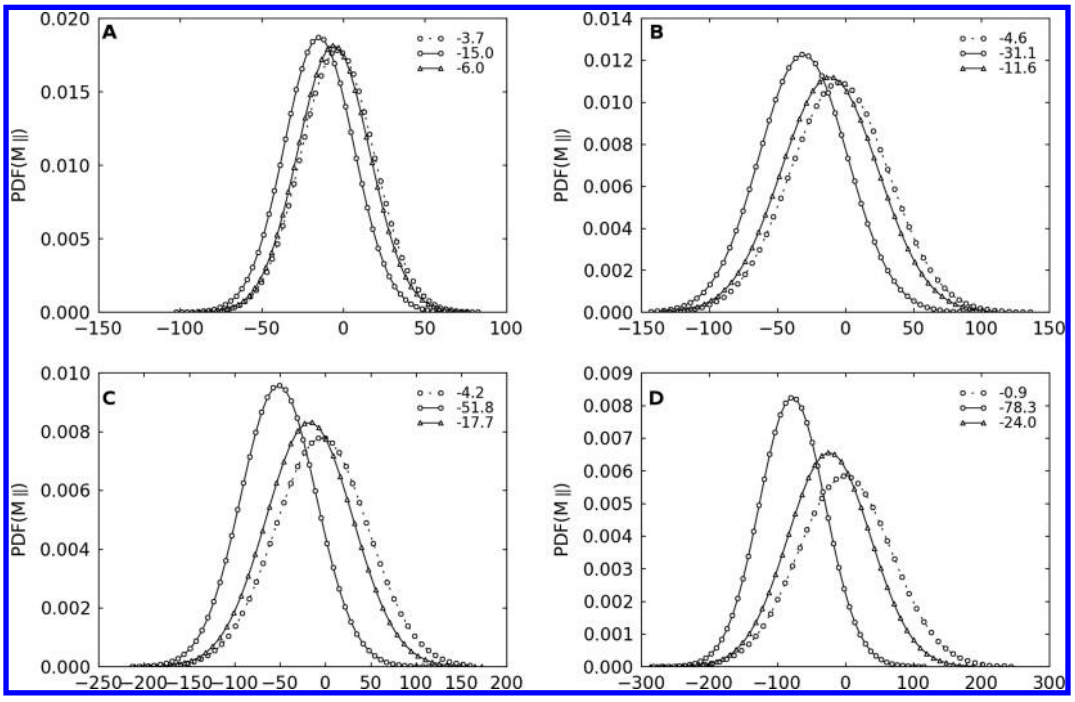

Figure 7. Projections of water layer dipole moments onto the direction of the alanine peptide dipole moment. (A) First hydration layer defined in the distance range within 0−2.5 Å from the peptide surface, (B) second layer within 2.5−5.0 Å, (C) third layer within 5.0−7.5 Å, and (D) fourth layer within 7.5−10.0 Å. Circle and dotted line, small system ($\varepsilon_{ext} = \infty$); circle and solid line, small system ($\varepsilon_{ext} = 70$); triangle and solid line, large system ($\varepsilon_{ext} = 70$). The average value of each distribution is reported in the legend.

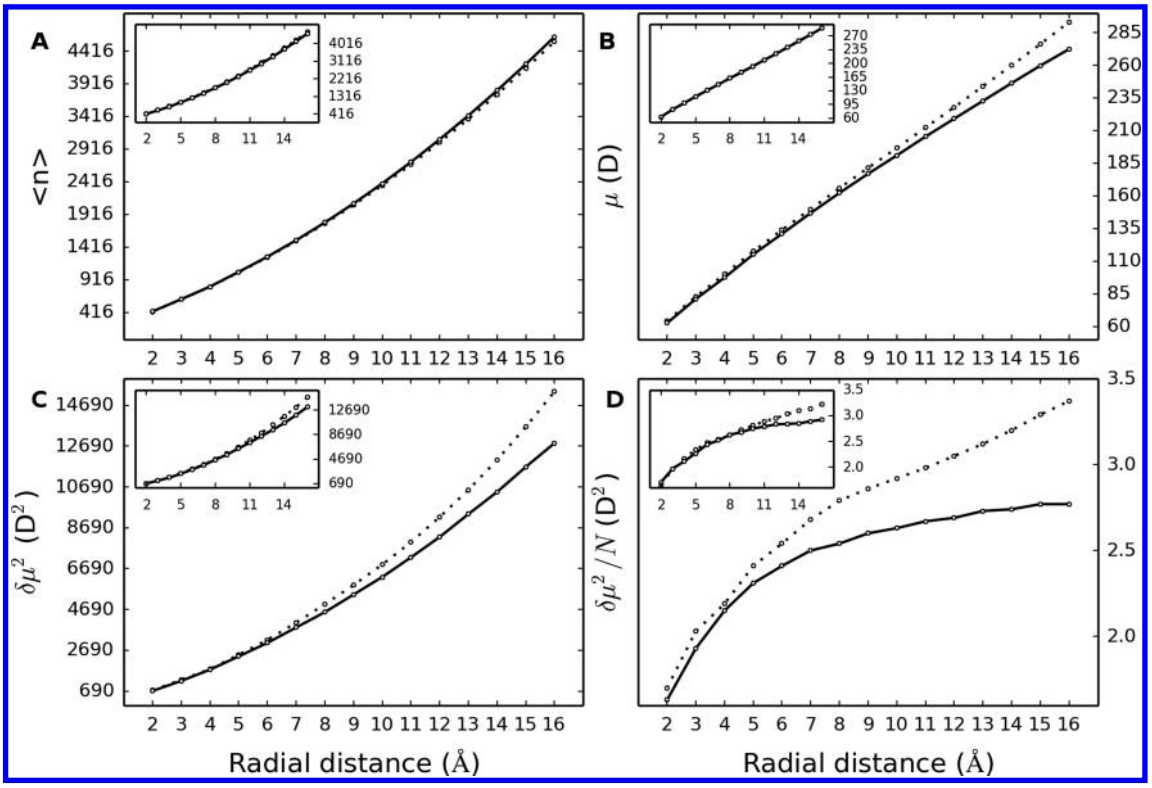

Figure 8. Dipole properties of the hydration layers around plastocyanin. (A) Average number of water molecules $\langle n \rangle$, (B) average dipole moment (μ), (C) dipole moment fluctuations ($\delta\mu^2$), and (D) normalized dipole moment fluctuations of the hydration layers as a function of the distance from the van der Waals surface of the protein (frozen system). Dotted and solid lines represent the simulations with ε_{ext} set to ∞ and 70, respectively. Data issuing from the free protein simulation are reported in the plot insets.

distance from the peptide van der Waals surface: for convenience, we selected three hydration layers of thickness 3.0, 6.0, and 9.0 Å from the peptide surface. Then, we have performed a dipole−dipole autocorrelation function analysis, as reported in Figure 6. Results show a consistent difference in the dipole relaxation rates between the two boundary regimes

DOI: 10.1021/jp511824t
J. Phys. Chem. A XXXX, XXX, XXX−XXX

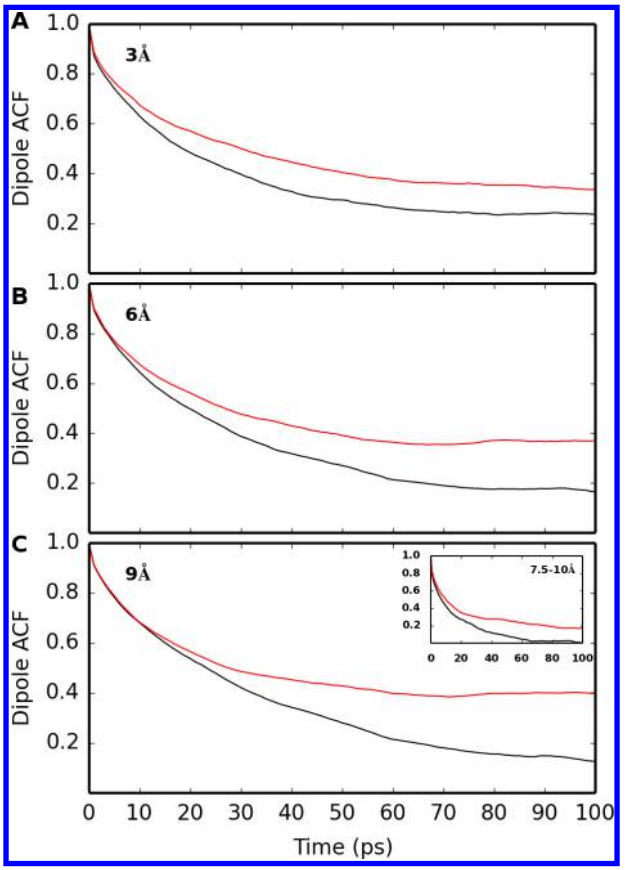

Figure 9. Reorientational autocorrelation functions of the water layer dipole moment issuing from regions of variable thickness (also indicated within each panel) from the protein surface: (A) hydration layer up to 3.0 Å from the protein surface, (B) hydration layer up to 6.0 Å, and (C) hydration layer up to 9.0 Å. In the inset of panel C, the same analysis is performed on a water layer with range 7.5−10.0 Å from the protein surface. Black line, system with $\varepsilon_{ext} = \infty$; red line, system with $\varepsilon_{ext} = 70$.

considered: a slower relaxation rate with $\varepsilon_{ext} = 70$ and a faster relaxation rate with $\varepsilon_{ext} = \infty$, the difference becoming larger at increasing water layer size (layer of 9 Å thickness, τ (70) = ∼70 ps; τ (∞) = ∼28 ps). In addition, the same analysis was performed on the large simulated system ($\varepsilon_{ext} = 70$), but in this case, no differences have been noticed (see Figure 6). To gain further insights into this unusual phenomenon, the average dipole moment was projected onto the alanine peptide dipole moment and the corresponding distribution evaluated for different hydration layers. As reported in Figure 7, an overpolarization of the water layers surrounding the peptide has been observed owing to the low-dielectric boundary conditions (small system, $\varepsilon_{ext} = 70$), as compared to tinfoil conditions ($\varepsilon_{ext} = \infty$). Such a spurious effect is largely reduced in the large system with $\varepsilon_{ext} = 70$, which provided dipole moment relaxation rates in good agreement with the high-conducting boundary ones: in other words, the significant water polarization observed with $\varepsilon_{ext} = 70$, and extending over several hydration layers, induced slower relaxation rates of the water layer dipoles and asymptotically nonzero ACFs at infinite time (see Figure 6).

3.4. Plastocyanin. Plastocyanin is a metalloprotein that acts as an electron carrier in natural photosynthesis. Previous simulation studies showed that the hydration layer around the protein is highly polarized.[70,71] Such a hydration layer, termed as the ferroelectric layer owing to its unusually large dipole moment and corresponding variance, plays an important role in stabilizing the charged interactions on the protein surface and does propagate up to 4−5 water shells into the bulk, thus producing an unconventional electrostatics at the solute−solvent interface. For such reasons, plastocyanin represents an optimal and intriguing test case for the computational investigation of the boundary condition effects.

In this work, plastocyanin has been simulated both with frozen and free atomic coordinates. The present choice was motivated, on one hand, by the same arguments discussed above for the alanine peptide (frozen system) and, on the other hand, by the interest to test results obtained with similar conditions (free protein) with respect to typical MD simulations of biosystems. Besides, with plastocyanin being a rather stable globular protein, we expected comparable, if not directly superimposable, results as issuing from the dipole analysis of the hydration layers in both cases. Results on the dipole properties of water layers around the van der Waals surface of the protein are collected in Figure 8. As usual, no differences have been observed in the standard analysis of the layer dipole moment with increasing thickness. On the contrary, an appreciable deviation between the DMF data, as issuing from high and low dielectric boundary conditions, already occurred at about ∼6 Å from the protein surface (Figure 8D), which roughly corresponds to the second water shell surrounding the protein. Furthermore, when protein motion was enabled, the DMF analysis led to an overall similar deviation between the two tested systems (see inset of Figure 8D), with a well-defined plateau characterizing again the nonstandard dielectric continuum ($\varepsilon_{ext} = 70$). Due to the dynamical change in the protein van der Waals surface, in this case, the DMF discrepancy manifests itself at a somewhat longer distance (∼11 Å) but still within the range accessible to modern spectroscopic techniques (15−20 Å).[10,11] Note that the specific details of the water DMF profile versus layer thickness are likely affected by the overall system size (e.g., simulation cell dimensions, number of water molecules, etc.), as noted in the preceding section; however, our findings seem to suggest that boundary effects on hydration layers are rather relevant for typical biosystem cell dimensions.

Similarly to the alanine peptide case, the dynamical features of the water layers around plastocyanin, as evaluated by the dipole ACFs, have shown a consistent faster relaxation with high-conducting boundary conditions with respect to low-dielectric ones (see Figure 9). Once more, higher amplitudes of the dipole fluctuations are accompanied by enhanced dipole relaxation rates. In addition, an overpolarization of the water layers surrounding the protein has been observed (see Figure 10) due to the low-dielectric boundary conditions (small system, $\varepsilon_{ext} = 70$), as compared to tinfoil conditions ($\varepsilon_{ext} = \infty$). A few considerations are due in order to rationalize the present results. The virtual periodicity imposed by PBCs can manifest itself through unwanted correlation effects in water dipole properties; however, the use of tinfoil conditions may effectively reduce or cancel such spurious effects in a typical sized system by enhancing the dipole moment fluctuations, which in turn repress long-range dipole correlations.

3.5. Self-Diffusion and Rotational Relaxation Times. All simulated systems consistently confirmed the sensitivity of the surrounding water DMFs to the dielectric boundary conditions applied. In order to examine the possible effects of the boundary conditions on the dynamical properties of water

DOI: 10.1021/jp511824t
J. Phys. Chem. A XXXX, XXX, XXX−XXX

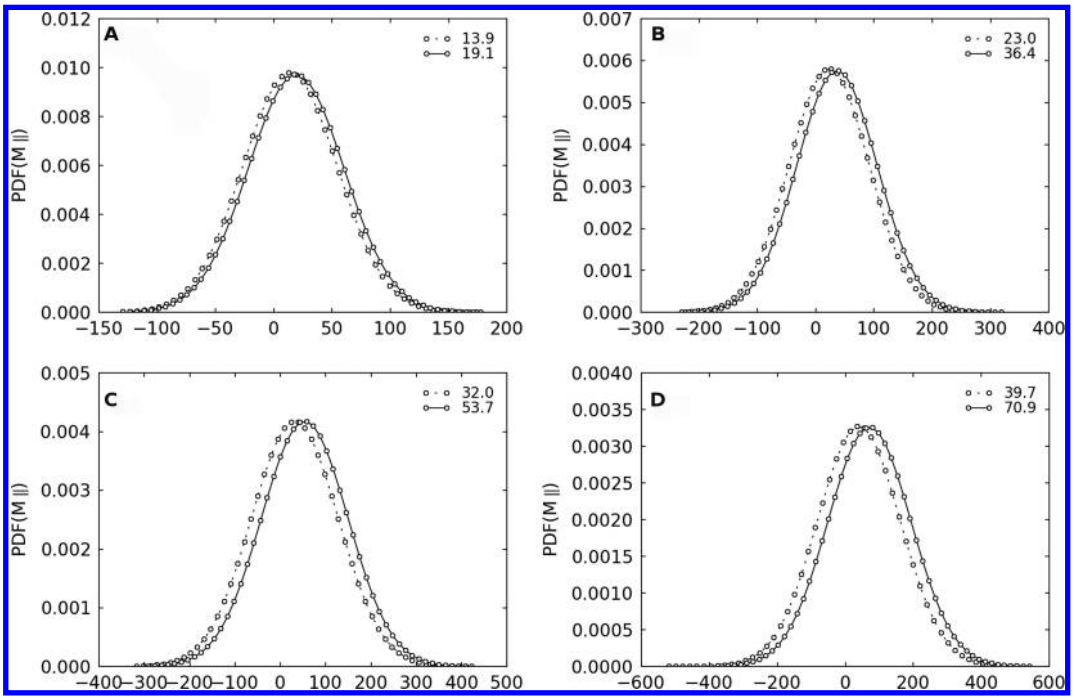

Figure 10. Projections of the water layer dipole moments onto the direction of the plastocyanin dipole moment. (A) First hydration layer defined in the distance range within 0−2.5 Å from the protein surface, (B) second layer within 2.5−5.0 Å, (C) third layer within 5.0−7.5 Å, and (D) fourth layer within 7.5−10.0 Å. Circle and dotted line, system with $\varepsilon_{ext} = \infty$; circle and solid line, system with $\varepsilon_{ext} = 70$. The average value of each distribution is reported in the legend.

Table 2. Dynamical Properties of Water Molecules around Alanine Peptide[a]

distance (Å)	D_∞	D_{70}	$\tau^{\mu}{}_\infty$	$\tau^{\mu}{}_{70}$	$\tau^{\perp}{}_\infty$	$\tau^{\perp}{}_{70}$
2.5	3.62	3.65	2.79	2.82	1.60	1.61
4.5	3.65	3.66	2.73	2.74	1.58	1.59
6.5	3.68	3.68	2.69	2.70	1.57	1.57
8.5	3.69	3.69	2.66	2.68	1.57	1.57

[a]Self-diffusion coefficient (D, 10^{-5} cm^2 s^{-1}), rotational relaxation time (ps) of water dipole (τ^{μ}), and normal to the water plane ($\tau^{\perp}$), calculated for water layers of increasing distance from the peptide surface.

Table 3. Dynamical Properties of Water Molecules around Plastocyanin[a]

distance (Å)	D_∞	D_{70}	$\tau^{\mu}{}_\infty$	$\tau^{\mu}{}_{70}$	$\tau^{\perp}{}_\infty$	$\tau^{\perp}{}_{70}$
2.5	4.39	4.33	3.39	3.63	1.66	1.78
5.0	4.43	4.42	3.17	3.21	1.58	1.61
7.5	4.49	4.47	3.03	3.06	1.53	1.54
10	4.51	4.49	2.95	2.97	1.50	1.51

[a]Dynamical properties of water molecules around alanine peptide. Self-diffusion coefficient (D, 10^{-5} cm^2 s^{-1}), rotational relaxation time (ps) of water dipole (τ^{μ}), and normal to the water plane ($\tau^{\perp}$), calculated for water layers of increasing distance from the protein surface.

molecules (i.e., at molecular level), we have evaluated the water self-diffusion coefficient and rotational relaxation time. These molecular properties computed on different water layers around the two considered biological systems described above are summarized in Tables 2 and 3. Results show that the mobility of the water molecules, calculated as a function of distance from the solute surface, is independent from the external dielectrics. Similarly, no difference has been observed in the reorientational relaxation times of the water dipole and the normal to the dipole vector. Overall, these findings indicate that molecular water properties are unaffected by any change of the boundary dielectric parameter, as previously noted in other studies.[65,68]

4. CONCLUSIONS

The present work highlights the effects of the external dielectric medium, usually an ignored parameter of the Ewald lattice sum method, in typical PBC simulations of aqueous solutions of biomolecules. In particular, our study focused on the analysis of the hydration layer properties, whose structural, dynamic, and dipole properties are nowadays accessible by various experimental techniques. To this end, three systems of increasing complexity have been systematically scrutinized at two different dielectric boundary conditions mimicking a highly conducting ($\varepsilon_{ext} = \infty$) and a low dielectric ($\varepsilon_{ext} = 70$) boundary medium. Overall, the obtained results consistently indicated that dipole moment fluctuations of the first solvation layers are rather sensitive to the boundary conditions applied. It has been shown that the extent of these effects generally depends on system size and solute dimension/flexibility: in general, the larger the system size, the smaller are the effects due to the external dielectrics on local solvent properties, since the boundary conditions become irrelevant at infinite dimension. In particular, with tinfoil boundary conditions, the solvent dipole fluctuations are largely enhanced even in local hydration layers within a few angstroms from the surface of biomolecules. On the other hand, the (normalized) dipole fluctuations smoothly converge to a thermodynamic limit under low-dielectric boundary conditions. Similarly, the external dielectric medium has induced spurious effects on the water layer polarization and dipole relaxation times: in this case, low-dielectric boundary conditions erroneously led to water overpolarization effects that, in turn, considerably reduced relaxation rates and/or

DOI: 10.1021/jp511824t
J. Phys. Chem. A XXXX, XXX, XXX−XXX

prevented the possibility of uncorrelated water dipole orientation expected at infinite time (asymptotically nonzero ACFs).

Overall, our study sheds some light on subtle, mostly ignored, boundary effects on aqueous solutions and cautions on the choice of appropriate boundary conditions and system size in order to minimize possible artifacts and obtain reliable estimates of water dipole properties. This is especially relevant in the modeling of hydration layers around biomolecules, though single molecule properties have not shown any dependence on the nature of the external dielectrics. While standard tinfoil conditions are confirmed as a generally safer choice in PBC/Ewald sum simulations, a physically sound modeling of the aqueous environment seems to be ensured only in the limiting case of large and truly uncorrelated systems.

AUTHOR INFORMATION

Corresponding Author

*E-mail: giuseppe.brancato@sns.it. Phone: +39 050509071. Fax: +39 050563513.

Present Address

§C.Z.: ASSCO, Università degli Studi di Roma *"La Sapienza"*, P.le Aldo Moro 5, 00185 Roma, Italy.

Notes

The authors declare no competing financial interest.

ACKNOWLEDGMENTS

This work was supported by MIUR through FIRB (Contract No. RBFR10DAK6 and RBFR12ETL5) and PRIN (Contract No. 2012SK7ASN) projects. The DREAMS Lab technical staff is kindly acknowledged for managing the computing facilities at SNS.

REFERENCES

(1) Solvent Influence on Protein Dynamics. In *Advances in Chemical Physics*, Brooks, C. L., III, Karplus, M., Pettitt, B. M., Eds.; John Wiley & Sons, Inc.:Hoboken, NJ, 2007; pp 137−174.

(2) Halle, B. Protein Hydration Dynamics in Solution: A Critical Survey. *Philos. Trans. R. Soc., B* **2004**, *359*, 1207−1328.

(3) Levy, Y.; Onuchic, J. N. Water Mediation in Protein Folding and Molecular Recognition. *Annu. Rev. Biophys. Biomol. Struct.* **2006**, *35*, 389−415.

(4) Bagchi, B. Water Dynamics in the Hydration Layer around Proteins and Micelles. *Chem. Rev.* **2005**, *105*, 3197−3219.

(5) Pal, S. K.; Zewail, A. H. Dynamics of Water in Biological Recognition. *Chem. Rev.* **2004**, *104*, 2099−2124.

(6) Bryant, R. G. The Dynamics of Water-Protein Interactions. *Annu. Rev. Biophys. Biomol. Struct.* **1996**, *25*, 29−53.

(7) Khoshtariya, D. E.; Hansen, E.; Leecharoen, R.; Walker, G. C. Probing Protein Hydration by the Difference O-H (O-D) Vibrational Spectroscopy: Interfacial Percolation Network Involving Highly Polarizable Water-Water Hydrogen Bonds. *J. Mol. Liq.* **2003**, *105*, 13−36.

(8) Zanni, M. T.; Hochstrasser, R. M. Two-Dimensional Infrared Spectroscopy: A Promising New Method for the Time Resolution of Structures. *Curr. Opin. Struct. Biol.* **2001**, *11*, 516−522.

(9) Pérez Lustres, J. L.; Kovalenko, S. A.; Mosquera, M.; Senyushkina, T.; Flasche, W.; Ernsting, N. P. Ultrafast Solvation of N-Methyl-6-Quinolone Probes Local Ir Spectrum. *Angew. Chem., Int. Ed.* **2005**, *44*, 5635−5639.

(10) Ebbinghaus, S.; Kim, S. J.; Heyden, M.; Yu, X.; Gruebele, M.; Leitner, D. M.; Havenith, M. Protein Sequence- and Ph-Dependent Hydration Probed by Terahertz Spectroscopy. *J. Am. Chem. Soc.* **2008**, *130*, 2374−2375.

(11) Ebbinghaus, S.; Kim, S. J.; Heyden, M.; Yu, X.; Heugen, U.; Gruebele, M.; Leitner, D. M.; Havenith, M. An Extended Dynamical Hydration Shell around Proteins. *Proc. Natl. Acad. Sci. U.S.A.* **2007**, *104*, 20749−20752.

(12) Sterpone, F.; Stirnemann, G.; Laage, D. Magnitude and Molecular Origin of Water Slowdown Next to a Protein. *J. Am. Chem. Soc.* **2012**, *134*, 4116−4119.

(13) Roy, S.; Bagchi, B. Free Energy Barriers for Escape of Water Molecules from Protein Hydration Layer. *J. Phys. Chem. B* **2012**, *116*, 2958−2968.

(14) Becker, O. M.; MacKerell, A. D., Jr.; Roux, B.; Watanabe, M. *Computational Biochemistry and Biophysics*, 1st ed.; Marcel Dekker, Inc.: New York, 2001; p 512.

(15) Dror, R. O.; Dirks, R. M.; Grossman, J. P.; Xu, H.; Shaw, D. E. Biomolecular Simulation: A Computational Microscope for Molecular Biology. *Annu. Rev. Biophys.* **2012**, *41*, 429−452.

(16) Schlick, T.; Collepardo-Guevara, R.; Halvorsen, L. A.; Jung, S.; Xiao, X. Biomolecular Modeling and Simulation: A Field Coming of Age. *Q. Rev. Biophys.* **2011**, *44*, 191−228.

(17) Leach, A. *Molecular Modelling: Principles and Applications*, 2nd ed.; Pearson Education: Harlow, England, 2001; p 784.

(18) Fox, T.; Kollman, P. A. The Application of Different Solvation and Electrostatic Models in Molecular Dynamics Simulations of Ubiquitin: How Well Is the X-Ray Structure "Maintained"? *Proteins* **1996**, *25*, 315−334.

(19) Schreiber, H.; Steinhauser, O. Molecular Dynamics Studies of Solvated Polypeptides: Why the Cut-Off Scheme Does Not Work. *Chem. Phys.* **1992**, *168*, 75−89.

(20) Schreiber, H.; Steinhauser, O. Cutoff Size Does Strongly Influence Molecular Dynamics Results on Solvated Polypeptides. *Biochemistry* **1992**, *31*, 5856−5860.

(21) Smith, P. E.; Pettitt, B. M. Peptides in Ionic Solutions: A Comparison of the Ewald and Switching Function Techniques. *J. Chem. Phys.* **1991**, *95*, 8430−8441.

(22) Bergdorf, M.; Peter, C.; Hünenberger, P. H. Influence of Cut-Off Truncation and Artificial Periodicity of Electrostatic Interactions in Molecular Simulations of Solvated Ions: A Continuum Electrostatics Study. *J. Chem. Phys.* **2003**, *119*, 9129−9144.

(23) de Vries, A. H.; Chandrasekhar, I.; van Gunsteren, W. F.; Hünenberger, P. H. Molecular Dynamics Simulations of Phospholipid Bilayers: Influence of Artificial Periodicity, System Size, and Simulation Time. *J. Phys. Chem. B* **2005**, *109*, 11643−11652.

(24) Hünenberger, P. H.; McCammon, J. A. Ewald Artifacts in Computer Simulations of Ionic Solvation and Ion−Ion Interaction: A Continuum Electrostatics Study. *J. Chem. Phys.* **1999**, *110*, 1856−1872.

(25) Hünenberger, P. H.; McCammon, J. A. Effect of Artificial Periodicity in Simulations of Biomolecules under Ewald Boundary Conditions: A Continuum Electrostatics Study. *Biophys. Chem.* **1999**, *78*, 69−88.

(26) Kastenholz, M. A.; Hünenberger, P. H. Influence of Artificial Periodicity and Ionic Strength in Molecular Dynamics Simulations of Charged Biomolecules Employing Lattice-Sum Methods. *J. Phys. Chem. B* **2004**, *108*, 774−788.

(27) Ye, X.; Cai, Q.; Yang, W.; Luo, R. Roles of Boundary Conditions in DNA Simulations: Analysis of Ion Distributions with the Finite-Difference Poisson-Boltzmann Method. *Biophys. J.* **2009**, *97*, 554−562.

(28) Smith, P. E.; Pettitt, B. M. Ewald Artifacts in Liquid State Molecular Dynamics Simulations. *J. Chem. Phys.* **1996**, *105*, 4289−4293.

(29) Yeh, I.-C.; Hummer, G. System-Size Dependence of Diffusion Coefficients and Viscosities from Molecular Dynamics Simulations with Periodic Boundary Conditions. *J. Phys. Chem. B* **2004**, *108*, 15873−15879.

(30) Pratt, L. R.; Haan, S. W. Effects of Periodic Boundary Conditions on Equilibrium Properties of Computer Simulated Fluids. Ii. Application to Simple Liquids. *J. Chem. Phys.* **1981**, *74*, 1873−1876.

(31) Boresch, S.; Steinhauser, O. Presumed Versus Real Artifacts of the Ewald Summation Technique: The Importance of Dielectric Boundary Conditions. *Ber. Bunsen-Ges.* **1997**, *101*, 1019−1029.

DOI: 10.1021/jp511824t
J. Phys. Chem. A XXXX, XXX, XXX−XXX

(32) Beglov, D.; Roux, B. Finite Representation of an Infinite Bulk System: Solvent Boundary Potential for Computer Simulations. *J. Chem. Phys.* **1994**, *100*, 9050−9063.
(33) Im, W.; Bernèche, S.; Roux, B. t. Generalized Solvent Boundary Potential for Computer Simulations. *J. Chem. Phys.* **2001**, *114*, 2924.
(34) Petraglio, G.; Ceccarelli, M.; Parrinello, M. Nonperiodic Boundary Conditions for Solvated Systems. *J. Chem. Phys.* **2005**, *123*, 044103.
(35) Warshel, A. A Microscopic Model for Calculations of Chemical Processes in Aqueous Solutions. *Chem. Phys. Lett.* **1978**, *55*, 454−458.
(36) Brancato, G.; Di Nola, A.; Barone, V.; Amadei, A. A Mean Field Approach for Molecular Simulations of Fluid Systems. *J. Chem. Phys.* **2005**, *122*, 154109.
(37) Brancato, G.; Rega, N.; Barone, V. Reliable Molecular Simulations of Solute-Solvent Systems with a Minimum Number of Solvent Shells. *J. Chem. Phys.* **2006**, *124*, 214505.
(38) Brancato, G.; Rega, N.; Barone, V. A Hybrid Explicit/Implicit Solvation Method for First-Principle Molecular Dynamics Simulations. *J. Chem. Phys.* **2008**, *128*, 144501.
(39) Miertuš, S.; Scrocco, E.; Tomasi, J. Electrostatic Interaction of a Solute with a Continuum. A Direct Utilizaion of Ab Initio Molecular Potentials for the Prevision of Solvent Effects. *Chem. Phys.* **1981**, *55*, 117−129.
(40) Tomasi, J.; Persico, M. Molecular Interactions in Solution: An Overview of Methods Based on Continuous Distributions of the Solvent. *Chem. Rev.* **1994**, *94*, 2027−2094.
(41) Del Ben, M.; VandeVondele, J.; Slater, B. Periodic Mp2, Rpa, and Boundary Condition Assessment of Hydrogen Ordering in Ice Xv. *J. Phys. Chem. Lett.* **2014**, *5*, 4122−4128.
(42) Berendsen, H.; Postma, J. *Interaction Models for Water in Relation to Protein Hydration* ; Dordrecht Reidel: Holland, 1981.
(43) Darden, T.; York, D.; Pedersen, L. Particle Mesh Ewald: An N·Log(N) Method for Ewald Sums in Large Systems. *J. Chem. Phys.* **1993**, *98*, 10089.
(44) Ballenegger, V. Communication: On the Origin of the Surface Term in the Ewald Formula. *J. Chem. Phys.* **2014**, *140*, 161102.
(45) Hess, B.; Bekker, H.; Berendsen, H. J. C.; Fraaije, J. G. E. M. Lincs: A Linear Constraint Solver for Molecular Simulations. *J. Comput. Chem.* **1997**, *18*, 1463−1472.
(46) Bussi, G.; Donadio, D.; Parrinello, M. Canonical Sampling through Velocity Rescaling. *J. Chem. Phys.* **2007**, *126*, 014101.
(47) Berendsen, H. J. C.; Grigera, J. R.; Straatsma, T. P. The Missing Term in Effective Pair Potentials. *J. Phys. Chem.* **1987**, *91*, 6269−6271.
(48) Jorgensen, W. L.; Chandrasekhar, J.; Madura, J. D.; Impey, R. W.; Klein, M. L. Comparison of Simple Potential Functions for Simulating Liquid Water. *J. Chem. Phys.* **1983**, *79*, 926−935.
(49) Pearlman, D. A.; Case, D. A.; Caldwell, J. W.; Ross, W. S.; Cheatham Iii, T. E.; DeBolt, S.; Ferguson, D.; Seibel, G.; Kollman, P. Amber, a Package of Computer Programs for Applying Molecular Mechanics, Normal Mode Analysis, Molecular Dynamics and Free Energy Calculations to Simulate the Structural and Energetic Properties of Molecules. *Comput. Phys. Commun.* **1995**, *91*, 1−41.
(50) Scott, W. R. P.; Hünenberger, P. H.; Tironi, I. G.; Mark, A. E.; Billeter, S. R.; Fennen, J.; Torda, A. E.; Huber, T.; Krüger, P.; van Gunsteren, W. F. The Gromos Biomolecular Simulation Program Package. *J. Phys. Chem. A* **1999**, *103*, 3596−3607.
(51) Xue, Y.; Okvist, M.; Hansson, O.; Young, S. Crystal Structure of Spinach Plastocyanin at 1.7 a Resolution. *Protein Sci.* **1998**, *7*, 2099−2105.
(52) De Kerpel, J. O.; Ryde, U. Protein Strain in Blue Copper Proteins Studied by Free Energy Perturbations. *Proteins* **1999**, *36*, 157−174.
(53) Duan, Y.; Wu, C.; Chowdhury, S.; Lee, M. C.; Xiong, G.; Zhang, W.; Yang, R.; Cieplak, P.; Luo, R.; Lee, T.; et al. A Point-Charge Force Field for Molecular Mechanics Simulations of Proteins Based on Condensed-Phase Quantum Mechanical Calculations. *J. Comput. Chem.* **2003**, *24*, 1999−2012.
(54) Van Der Spoel, D.; Lindahl, E.; Hess, B.; Groenhof, G.; Mark, A. E.; Berendsen, H. J. C. Gromacs: Fast, Flexible, and Free. *J. Comput. Chem.* **2005**, *26*, 1701−1718.
(55) Allen, M. P.; Tildesley, D. J. *Computer Simulation of Liquids*; Oxford University Press: New York, 1989; p 412.
(56) Anderson, J.; Ullo, J. J.; Yip, S. Molecular Dynamics Simulation of Dielectric Properties of Water. *J. Chem. Phys.* **1987**, *87*, 1726−1732.
(57) van der Spoel, D.; van Maaren, P. J.; Berendsen, H. J. C. A Systematic Study of Water Models for Molecular Simulation: Derivation of Water Models Optimized for Use with a Reaction Field. *J. Chem. Phys.* **1998**, *108*, 10220.
(58) Bizzarri, A. R.; Cannistraro, S. Molecular Dynamics of Water at the Protein−Solvent Interface. *J. Phys. Chem. B* **2002**, *106*, 6617−6633.
(59) Pettersen, E. F.; Goddard, T. D.; Huang, C. C.; Couch, G. S.; Greenblatt, D. M.; Meng, E. C.; Ferrin, T. E. Ucsf Chimera–a Visualization System for Exploratory Research and Analysis. *J. Comput. Chem.* **2004**, *25*, 1605−1612.
(60) Hunter, J. D. Matplotlib: A 2d Graphics Environment. *Comput. Sci. Eng.* **2007**, *9*, 90−95.
(61) Kirkwood, J. G. The Dielectric Polarization of Polar Liquids. *J. Chem. Phys.* **1939**, *7*, 911−919.
(62) Kirkwood, J. G.; Shumaker, J. B. The Influence of Dipole Moment Fluctuations on the Dielectric Increment of Proteins in Solution. *Proc. Natl. Acad. Sci. U.S.A.* **1952**, *38*, 855−862.
(63) Neumann, M. Dipole Moment Fluctuation Formulas in Computer Simulations of Polar Systems. *Mol. Phys.* **1983**, *50*, 841−858.
(64) Neumann, M. The Dielectric Constant of Water. Computer Simulations with the Mcy Potential. *J. Chem. Phys.* **1985**, *82*, 5663−5672.
(65) De Leeuw, S. W.; Perram, J. W.; Smith, E. R. Computer Simulation of the Static Dielectric Constant of Systems with Permanent Electric Dipoles. *Annu. Rev. Phys. Chem.* **1986**, *37*, 245−270.
(66) Neumann, M. Dielectric Relaxation in Water. Computer Simulations with the Tip4p Potential. *J. Chem. Phys.* **1986**, *85*, 1567−1580.
(67) Bratko, D.; Daub, C. D.; Luzar, A. Field-Exposed Water in a Nanopore: Liquid or Vapour? *Phys. Chem. Chem. Phys.* **2008**, *10*, 6807−6813.
(68) De Leeuw, S. W.; Perram, J. W. Computer Simulation of Ionic Systems. Influence of Boundary Conditions. *Physica A* **1981**, *107*, 179−189.
(69) Höchtl, P.; Boresch, S.; Bitomsky, W.; Steinhauser, O. Rationalization of the Dielectric Properties of Common Three-Site Water Models in Terms of Their Force Field Parameters. *J. Chem. Phys.* **1998**, *109*, 4927−4937.
(70) LeBard, D. N.; Matyushov, D. V. Glassy Protein Dynamics and Gigantic Solvent Reorganization Energy of Plastocyanin. *J. Phys. Chem. B* **2008**, *112*, 5218−5227.
(71) LeBard, D. N.; Matyushov, D. V. Ferroelectric Hydration Shells around Proteins: Electrostatics of the Protein-Water Interface. *J. Phys. Chem. B* **2010**, *114*, 9246−9258.

DOI: 10.1021/jp511824t
J. Phys. Chem. A XXXX, XXX, XXX−XXX